

TURUN YLIOPISTON JULKAISUJA
ANNALES UNIVERSITATIS TURKUENSIS

SARJA - SER. A I OSA - TOM. 439

ASTRONOMICA - CHEMICA - PHYSICA - MATHEMATICA

**NON-MARKOVIAN DYNAMICS AND
THE QUANTUM-TO-CLASSICAL
TRANSITION FOR QUANTUM
BROWNIAN MOTION**

by

Janika Paavola

TURUN YLIOPISTO
UNIVERSITY OF TURKU
Turku 2012

From

Department of Physics and Astronomy
University of Turku
Finland

Supervised by

Dr. Sabrina Maniscalco Reader in Physics School of Engineering and Physical Sciences Heriot-Watt University Edinburgh, UK	Department of Physics and Astronomy University of Turku Finland
---	---

Reviewed by

Dr. Matteo Scala Senior Research Associate Dipartimento di Scienze Fisiche ed Astronomiche Università di Palermo Italia	Dr. Stefano Olivares Senior Research Associate Dipartimento di Fisica Università degli Studi di Milano Italia
---	---

Opponent

Prof. Andreas Buchleitner
Professor of Theoretical Physics
Physikalisches Institut
Albert-Ludwigs-Universität Freiburg
Germany

ISBN 978-951-29-5008-9 (print)
ISBN 978-951-29-5009-6 (pdf)
ISSN 0082-7002
Painosalama Oy - Turku, Finland 2012

Acknowledgments

The Thesis at hand summarizes my scientific work done in the Department of Physics and Astronomy at the University of Turku during the years 2008-2012.

I wish to thank my supervisor Dr. Sabrina Maniscalco for her careful guidance during these four years. Her enthusiasm regarding both scientific and public outreach activities has made working in the group of Open Quantum Systems and Entanglement a true pleasure.

From the scientific point of view, I wish to thank especially all my co-authors, Dr. Jyrki Piilo, Prof. Kalle-Antti Suominen, Prof. Matteo G. A. Paris and Dr. Michael J. W. Hall for fruitful collaboration and pleasant scientific discussions.

My warmest thanks goes to all my friends and colleagues of "the corridor". I enjoyed very much spending time with them both in the office and outside of University.

I want to thank my family for their all-round support and interest in my work. In particular I am deeply grateful for my husband Ville for his support and for being such a constant source of inspiration.

Finally, I gratefully acknowledge financial support from Vilho, Yrjö and Kalle Väisälä Foundation, Magnus Ehrnrooth Foundation, Emil Aaltonen Foundation, Turku University Foundation and the Finnish Concordia Fund.

Contents

List of publications	v
1 Introduction	1
2 Open quantum systems	4
2.1 The model: quantum Brownian motion	6
3 Nonclassicality of quantum states	9
3.1 The Wigner function	9
3.2 Other quasiprobability distribution functions	10
4 Transition from quantum to classical	13
4.1 Environment induced decoherence	13
4.2 The life and death of the Schrödinger-cat state	14
4.3 Time evolution of nonclassicality	15
4.3.1 Peak of the interference fringe	15
4.3.2 Nonclassical depth	17
4.3.3 Negativity of the Wigner function	19
4.3.4 Vogel criterion	19
4.3.5 Klyshko criterion	22
4.4 Emergence of classicality	24
5 Structured reservoirs and reservoir memory	26
5.1 Non-Markovian dynamics	26
5.2 Structured reservoirs	27
6 Decoherence and dissipation under different reservoirs	29
6.1 Solution for the equation of motion	29
6.2 Decay channels	30
6.3 Non-Markovian energy transfer	31
6.4 Markovian limit and thermalization dynamics	32
6.5 Decoherence	33
6.6 Non-Markovian squeezing	34
7 Decoherence control	36
7.1 Reservoir engineering	36
7.2 The quantum Zeno effect	38

8 Conclusions	42
References	43

Abstract

In this Thesis I discuss the dynamics of the quantum Brownian motion model in harmonic potential. This paradigmatic model has an exact solution, making it possible to consider also analytically the non-Markovian dynamics.

The issues covered in this Thesis are themed around decoherence. First, I consider decoherence as the mediator of quantum-to-classical transition. I examine five different definitions for nonclassicality of quantum states, and show how each definition gives qualitatively different times for the onset of classicality. In particular I have found that all characterizations of nonclassicality, apart from one based on the interference term in the Wigner function, result in a finite, rather than asymptotic, time for the emergence of classicality.

Second, I examine the diverse effects which coupling to a non-Markovian, structured reservoir, has on our system. By comparing different types of Ohmic reservoirs, I derive some general conclusions on the role of the reservoir spectrum in both the short-time and the thermalization dynamics. Finally, I apply these results to two schemes for decoherence control. Both of the methods are based on the non-Markovian properties of the dynamics.

List of publications

This Thesis consists of an introductory part, followed by four research publications.

- I *Environment-dependent dissipation in quantum Brownian motion*
J. Paavola, K.-A. Suominen, J. Piilo, and S. Maniscalco
Physical Review A **79** (2009) 052120 (10 pages).
- II *Non-Markovian reservoir-dependent squeezing*
J. Paavola
Physica Scripta **T140** (2010) 014030 (4 pages).
- III *Decoherence control in different environments*
J. Paavola and S. Maniscalco
Physical Review A **82** (2010) 012114 (8 pages).
- IV *Finite-time quantum-to-classical transition for a Schrödinger-cat state*
J. Paavola, M. J. W. Hall, M. G. A. Paris, and S. Maniscalco
Physical Review A **84** (2011) 012121 (9 pages).

1 Introduction

Quantum theory describes physical phenomena that can most readily be observed at the atomic scale. One of the characteristic features of quantum physics is a type of nonclassical correlation, entanglement, which may seem bizarre but has nevertheless been verified in countless experiments [1–3]. Experiments have also confirmed another key aspect of quantum theory, quantum superpositions. In these experiments a particle has seemingly two mutually exclusive properties, like position to the right and to the left of a reference point simultaneously [4]. All conceivable superpositions of two possible system states can exist, and the number of these superpositions is vastly greater than the number of classically acceptable states. Although such superpositions have been verified by experiments on the microscopic scale, and also for bigger fullerene molecules [5], they are not routinely observable on the truly macroscopic scale. Why are quantum superposition of macroscopically distinguishable states not observed in the classical world where we live? This question is also known as the quantum measurement problem.

Currently the prevailing explanation is environment induced decoherence (EID) [6]. EID is seen as the cause of the so called quantum-to-classical transition, which transforms the non-local, entangled macroscopic state or the single-particle superposition state, into a classically acceptable, local state. The theory of open quantum systems is the theoretical framework behind EID, since it explicitly takes into account the environment our system of interest is interacting with [7]. In principle, all quantum systems are open, that is, interacting with their surroundings. Open quantum systems are, however, much more difficult to deal with than the common textbook example of closed systems following the Schrödinger equation.

When the interaction with the environment is taken into account, the dynamics is not unitary anymore and the equation of motion rarely has an analytic solution. Therefore one often has to make approximations in order to obtain analytical results. The two most common approximations are the Born or weak coupling approximation, and the Markov approximation. The former assumes that the system and the reservoir are not interacting very strongly, while the latter one neglects the short time correlations between the system and the reservoir.

Although such approximations are sometimes useful, they do not hold for certain important situations, for example with atoms decaying in photonic band gap materials [8], or atom lasers [9].

In this thesis I study the quantum Brownian motion model, describing

the evolution of a quantum harmonic oscillator coupled to a heat bath at T -temperature, for which an exact master equation with exact solution exists [10]. In particular, I use this model to address the problem of the transition from quantum to classical, and also to examine the effects that different structured environments have on the system. The latter problem is useful for quantum technologies, since decoherence can be fought in various ways by the manipulation of the artificial reservoir.

The former issue, namely the quantum-to-classical transition, is approached by asking how do we define nonclassical and classical states and determine how the dynamical evolution drives an initially nonclassical state into a classical-like state? More precisely, we consider a superposition of two coherent states, and compare five different nonclassicality measures to characterize its nonclassicality. We find that the prevailing conception that the bigger the wave packet separation in the initially nonclassical state, the faster decoherence breaks it apart, is not always true. This statement was based on the properties of the Wigner function interference terms, which are present for a quantum superposition state, and are later washed away by decoherence. However, the interference terms do not have any operatorial interpretation. They are not a property of the system that can be measured, rather one has to reconstruct the whole density matrix, and deduce the signs of nonclassicality from there in the form of Wigner function fringes.

Many other characteriztons for what determines a nonclassical (and therefore also classical) state exist in the literature. In this thesis I present four of them, each having an operatorial, directly measurable, indication. We show that by adopting different nonclassicality definitions, larger superpositions do not always decohere faster. Also, the nature of quantum-to-classical transition changes drastically. With these new measures, the transition occurs at a finite time, much like entanglement sudden death, an effect found very recently, where quantum correlations suddenly disappear completely [11]. Following the Wigner function fringes, the state would approach a classical state only asymptotically.

Another main topic in this Thesis is related to environments with structure. Structured environments induce often dynamics that are non-Markovian. The short-time correlations present in the system induce a back-flow of information from the reservoir to the system. In the theory of open quantum systems, non-Markovian effects have been under lively discussion during the last decade. Non-Markovianity as a phenomenon is not completely understood yet due to the challenges related to solving the master equations. Even the definition of

non-Markovianity has been under much debate, with many different proposed non-Markovianity measures [12–15].

In particular I examine the phenomena of decoherence, dissipation or energy transfer, and squeezing of a quantum harmonic oscillator coupled to a heat bath. We have shown analytically, that there exists a correspondence between certain types of decoherence dynamics and the reservoir structure. Due to this connection, we can propose ways to reduce these harmful effects by either controlling experimentally the reservoir structure, or the system coupling with the reservoir. One approach is to choose one’s experimental implementation in such a way, that the reservoir leads to optimal preservation of coherences.

Another possibility in controlling decoherence, is to take advantage of the quantum Zeno effect, which owing to its original meaning in ancient Greek, essentially consists of stopping or slowing down the dynamics by very frequent measurements. This can be implemented by simply rapidly turning on and off the coupling in a trapped ion context, for example [16]. The quantum Zeno effect is a non-Markovian effect, arising from the quadratic short-time dynamics of the open system.

The structure of this thesis is the following. In Chapter 2 I introduce basic concepts of open quantum systems, and present the ubiquitous model used throughout the thesis. Chapter 3 introduces the phase space description of the quantum state, i.e., the quasiprobability distribution functions, the most familiar of them being the Wigner function. In Chapter 4 I present the different nonclassicality definitions, all based on the properties of the quasiprobability distributions introduced in the previous chapter, and I use these definitions to describe the dynamical evolution of an initially highly nonclassical state. In Chapter 5 I cover in more detail the role of structured reservoirs as the inducers of non-Markovianity. In Chapter 6 I describe how different structured reservoirs induce different types of decoherence and dissipation. Chapter 7 is dedicated to the topic of decoherence control via two types of experimental manipulations of the reservoir. Finally, in Chapter 8 I draw conclusions.

2 Open quantum systems

Open quantum systems are quantum systems that interact with their surroundings [7,17]. The theory of open quantum systems has recently received renewed attention due to the fact that emerging quantum technologies are heavily affected by the detrimental effects of the environment, such as decoherence and dissipation. To cope with these destructive effects, a better understanding of their sources and microscopic origin is needed, and this can often be accomplished using the powerful approaches of the theory of open quantum systems.

Open quantum systems are an inherent part of the fundamentals of quantum theory, because in reality all quantum systems are open. Under certain conditions it is possible to approximate a quantum system to be closed, therefore neglecting the effects of the environment. In practice open quantum system approach is used in a variety of fields, including quantum optics [18], condensed matter physics [19] and quantum chemistry [20,21].

Open quantum systems are described by master equations, which are the equations of motion for the density matrix of the open system. They are usually derived starting from the initially closed total system and then tracing out the environmental degrees of freedom to obtain the time evolution of the system of interest only. Their solution is often far from trivial, and therefore the need to make simplifying approximations arises.

The most common of these approximations is the Born or weak coupling approximation. It assumes that the coupling between the system and the reservoir is weak compared to the system energy. This makes it possible to neglect all but second order terms in the master equation, simplifying the problem. In this Thesis I will always assume weak coupling. The second common assumption is to neglect short-time correlations between the system and the environment. This is called the Markovian approximation.

In addition, it is usually also assumed that the system and the environment are initially uncorrelated. For weak system–reservoir coupling assuming factorized initial condition is a justified approximation.

Due to the dissipative coupling with the environment, open quantum systems do not follow unitary evolution. This causes the dynamics to be irreversible. The most general form of this irreversible evolution is given in terms of a Markovian master equation in the Lindblad form,

$$\frac{d\rho(t)}{dt} = -i[H_S, \rho(t)] + \sum_k \gamma_k \left(A_k \rho(t) A_k^\dagger - \frac{1}{2} A_k^\dagger A_k \rho(t) - \frac{1}{2} \rho(t) A_k^\dagger A_k \right), \quad (1)$$

where the first term on the right hand side gives the unitary evolution induced by system Hamiltonian H_S . The second term is the dissipator. Here γ_k denote the positive relaxation rates for different decay channels k , and A_k are known as the jump operators. An example of non-Markovian dynamics is given by the time-local non-Markovian master equation, which is identical to Eq. (1) with the exception that γ_k are time-dependent and can take temporarily negative values. During the times the relaxation rates are negative, the previous state of the system can be temporarily restored [22, 23].

These transient effects, described by non-Markovian dynamics, generally occur at short time scales. When the time scale of interest is sufficiently long and the coupling between system and reservoir is weak, the non-Markovian effects can be neglected. Under appropriate conditions, however, they are the key ingredient to slowing down decoherence by the so-called quantum Zeno effect [24]. I will describe in more detail the quantum Zeno effect in Chapter 7.

The best understood class of open quantum systems are Markovian systems, as described by Eq. (1), for example. The dynamics of the density matrix of a Markovian system is described by a dynamical map $V(t) : \rho(t) = V(t)\rho(0)$, which satisfies the positivity, complete positivity (CP) and semigroup properties [17]. The positivity condition ensures that all positive operators are mapped into positive operators. The CP guarantees that density operators in all possible extended Hilbert spaces are mapped into density operators in the same extended Hilbert space. Finally, the semigroup property means that $V(t_1)V(t_2) = V(t_1 + t_2)$.

Complete positivity is an important requirement for the physicality of the quantum state evolution. The celebrated Lindblad theorem [25] tells us that all Markovian master equations that can be cast in the so called Lindblad form (see Eq. (1)) are completely positive and trace preserving [26].

However, complete positivity is valid also for exact (and therefore non-Markovian) master equations with the factorized initial condition, which are then described by completely positive dynamical maps [27, 28]. In this Thesis the factorized initial condition and weak coupling are always assumed. In the following, when making approximations to the exact master equation, we will consider only the dynamical regimes consistent with these approximations, thus guaranteeing complete positivity of the dynamics.

In this thesis I focus on an open, continuous variable quantum system that is coupled to a heat bath, namely the quantum Brownian motion model. In the next section I will describe this model.

2.1 The model: quantum Brownian motion

The model system used throughout the Thesis is known as the quantum Brownian motion or the damped harmonic oscillator model [7]. It consists of a quantum harmonic oscillator linearly coupled through position with a reservoir consisting of an infinite chain of independent quantum harmonic oscillators.

The total microscopic Hamiltonian is

$$H = H_S + H_E + H_{int}, \quad (2)$$

where the Hamiltonians of the system oscillator, environment and interaction read ¹

$$H_S = \omega_0 \left(a^\dagger a + \frac{1}{2} \right), \quad (3)$$

$$H_E = \sum_{n=0}^{\infty} \omega_n \left(b_n^\dagger b_n + \frac{1}{2} \right), \quad (4)$$

$$H_{int} = \frac{1}{\sqrt{2}} (a + a^\dagger) \sum_n k_n (b_n + b_n^\dagger). \quad (5)$$

As usual, a (a^\dagger) and b_n (b_n^\dagger) are the annihilation (creation) operators of the system and the environment oscillators, respectively, ω_0 and ω_n are the frequencies of the system and the environment oscillators. In the continuum limit the coupling constants k_n , which describe the coupling strength between each mode of the reservoir and the system oscillator, form the reservoir spectrum: $J(\omega) = \sum_n k_n \delta(\omega - \omega_n) / (2m_n \omega_n)$, with m_n the mass of the n -th environmental oscillator [7].

The quantum Brownian motion (QBM) model is one of the few models in the theory of open quantum systems where an exact master equation with an exact solution exists. Assuming only that the system and the environment are initially uncorrelated, $\rho_{total} = \rho_S \otimes \rho_E$, one derives the master equation describing the dynamics of the reduced system of interest. This is known as the Hu-Paz-Zhang master equation and it is derived starting from the total Hamiltonian in Eq. (2) and tracing out the environment [10, 29, 30]. In the

¹In this Thesis natural units are used so that $\hbar = 1$.

interaction picture, the Hu-Paz-Zhang master equation reads as follows

$$\begin{aligned} \frac{d\rho(t)}{dt} = & -\Delta(t)[X, [X, \rho(t)]] + \Pi(t)[X, [P, \rho(t)]] + \frac{i}{2}r(t)[X^2, \rho(t)] \\ & - i\gamma(t)[X, \{P, \rho(t)\}], \end{aligned} \quad (6)$$

where $\rho(t)$ is the density matrix for the system oscillator, $X = (a + a^\dagger)/\sqrt{2}$ and $P = i(a^\dagger - a)/\sqrt{2}$. The coefficients $\Delta(t)$ and $\Pi(t)$ are the normal and anomalous diffusion coefficients, $\gamma(t)$ is the dissipation coefficient and $r(t)$ gives the time-dependent frequency shift [29]. Under weak coupling assumption the time-dependent coefficients can be written down in closed form

$$\Delta(t) = \int_0^t \kappa(\tau) \cos(\omega_0\tau) d\tau, \quad (7)$$

$$\gamma(t) = \int_0^t \mu(\tau) \sin(\omega_0\tau) d\tau, \quad (8)$$

$$\Pi(t) = \int_0^t \kappa(\tau) \sin(\omega_0\tau) d\tau, \quad (9)$$

$$r(t) = \int_0^t \mu(\tau) \cos(\omega_0\tau) d\tau, \quad (10)$$

where $\kappa(\tau) = g^2 \langle \{E(\tau), E(0)\} \rangle$ and $\mu(\tau) = ig^2 \langle [E(\tau), E(0)] \rangle$ are the noise and dissipation kernels with g the dimensionless coupling constant, respectively [29]. For sufficiently weak couplings and in the high temperature regime $r(t)$ and $\Pi(t)$ can be neglected [10]. In this regime, and for time scales that are much shorter than thermalization time, an approximate master equation can be written as [31]

$$\begin{aligned} \frac{d\rho(t)}{dt} = & -\frac{\Delta(t) + \gamma(t)}{2} [2a\rho(t)a^\dagger - a^\dagger a\rho(t) - \rho(t)a^\dagger a] \\ & + \frac{\Delta(t) - \gamma(t)}{2} [2a^\dagger \rho(t)a - aa^\dagger \rho(t) - \rho(t)aa^\dagger] \\ & + \frac{\Delta(t) - \gamma(t)}{2} e^{-2i\omega_0 t} [2a\rho(t)a - a^2\rho(t) - \rho(t)a^2] \\ & + \frac{\Delta(t) - \gamma(t)}{2} e^{2i\omega_0 t} [2a^\dagger \rho(t)a^\dagger - (a^\dagger)^2 \rho(t) - \rho(t)(a^\dagger)^2]. \end{aligned} \quad (11)$$

Also this master equation is local in time. That is, it does not contain a memory kernel keeping track of all the past history of the system. Instead of a memory kernel, the memory of the interaction between the system and the environment is stored in the time-dependent coefficients, $\Delta(t)$ and $\gamma(t)$.

Often in the literature non-Markovian master equations are associated with memory kernel master equations. The Hu-Paz-Zhang master equation is time local but exact, thus describing also the non-Markovian dynamics. This example shows that non-Markovian master equations do not need to be described by integro-differential equations containing a memory kernel. Also analytical results exist confirming this phenomenon [32].

The master equation (11) can be further simplified by noticing that the last two terms in Eq. (11) oscillate quickly compared to the first two terms. In secular approximation we coarse grain over the time scales of the order $1/\omega_0$, and as a result the rapidly oscillating terms average out to zero. We will see later in Section 5.2 that the validity of the secular approximation, if one wants to observe the short time non-Markovian dynamics, depends strongly on certain reservoir parameters. In contrast, some observables, like the mean energy of the system, which we will consider in Chapter 6, are completely immune to the effect of the secular approximation. The simplest master equation for Hamiltonian (2) can thus be written as

$$\begin{aligned} \frac{d\rho(t)}{dt} = & -\frac{\Delta(t) + \gamma(t)}{2} [2a\rho(t)a^\dagger - a^\dagger a\rho(t) - \rho(t)a^\dagger a] \\ & + \frac{\Delta(t) - \gamma(t)}{2} [2a^\dagger \rho(t)a - aa^\dagger \rho(t) - \rho(t)aa^\dagger], \end{aligned} \quad (12)$$

where the diffusion and dissipation coefficients can be written, to second order in perturbation theory and assuming that the reservoir is stationary, as

$$\begin{aligned} \Delta(t) = & 2 \int_0^t dt' \int_0^\infty d\omega J(\omega) \left[N(\omega) + \frac{1}{2} \right] \cos(\omega t') \cos(\omega_0 t'), \\ \gamma(t) = & 2 \int_0^t dt' \int_0^\infty d\omega \frac{J(\omega)}{2} \sin(\omega t') \sin(\omega_0 t'), \end{aligned} \quad (13)$$

with $N(\omega) = (e^{\omega/k_B T} - 1)^{-1}$ the average number of reservoir thermal excitations, k_B the Boltzmann constant, and T the reservoir temperature.

Some of the states of the quantum harmonic oscillator have properties that can be meaningfully associated to classical states of the phase space, while others have more pronounced quantum features, void of any resemblance to classical states. Distinguishing between quantum and classical states is crucial for the study of decoherence, and quantum-to-classical transition, which are the main topics of this Thesis. In the next chapter I will present the definitions of quantum and classical states for the quantum harmonic oscillator.

3 Nonclassicality of quantum states

In classical mechanics, particles move along trajectories in phase space having definite position and momentum at all times. The uncertainty principle states that quantum mechanical objects cannot be described by well-defined points in phase space. We can still represent a quantum state in phase space by using certain distributions, like the Wigner function, that resemble classical probability distributions. In this formalism any deviation from a classical distribution function, such as negativities, may be considered as a sign of nonclassicality.

Coherent state is considered as the most classical-like state, because in the phase space representation, given by a Wigner function, it minimizes the uncertainties both in position and momentum thus resembling a point as close as the uncertainty principle allows. The Wigner function for a coherent state is a finite, normalized and positive distribution, satisfying all the requirements for a proper probability distribution. Many other states, however, have Wigner functions that do not fulfill these requirements. They can acquire negative values, for example. This is considered as a sign of nonclassicality.

Giving a more accurate characterization of classical and nonclassical quantum states of the quantum harmonic oscillator is an important and still open task. Complete characterization of nonclassical states, and in particular finding a measurable criteria to determine the degree of nonclassicality, is important for the newly emerging quantum technologies that rely on the quantum properties as their driving engine. For quantum optical systems, entanglement can be generated with a beam splitter, if the input state (the other input being the vacuum $|0\rangle$) is nonclassical [33, 34]. Therefore, the capability to measure the amount of nonclassicality in a system is highly desired for the generation of entanglement, which can then be used for quantum information purposes [35].

In quantum state characterization and for defining nonclassicality, many approaches rely on the properties of quasiprobability distribution functions. With this in mind, I will now introduce commonly used distribution functions, starting from the most familiar one, the Wigner function.

3.1 The Wigner function

Although joint measurement of position and momentum is not possible due to the non-commutativity of these operators, E. Wigner introduced as early as in 1932 [36], the Wigner function that is *formally* equivalent to the probability distribution for a joint measurement of position and momentum. The marginal

integrals of the Wigner function give the position and momentum probability distributions. From the definition of the Wigner function [92],

$$W(\beta) = \int \frac{d^2\xi}{\pi} e^{\beta\xi^* - \beta^*\xi} \chi(\xi), \quad (14)$$

where the so called Wigner characteristic function reads

$$\chi(\xi) = \text{Tr}[\rho e^{\xi\hat{a}^\dagger - \xi^*\hat{a}}], \quad (15)$$

it is clear that it contains the full information of the state of the system, ρ , because the Fourier transform in Eq. (14) is fully invertible.

The Wigner function has properties similar to those of any probability distribution, such as being normalized to unity, and having real number values. Differently from proper probability distributions, however, it can also take negative values. The Wigner function is therefore denoted as a quasiprobability distribution. Despite this, the Wigner function is a useful tool in quantum optics for representing quantum states. For example, squeezing is intuitively shown as the narrowing of the Wigner function width in a given direction.

The characteristic function in Eq. (15) is called symmetric, because the operators a and a^\dagger are ordered symmetrically. For different ordering, such as $a^n a^{\dagger m}$ or $a^{\dagger n} a^m$, we can define other quasiprobability distribution functions, such as the normally ordered and the anti-normally ordered distribution functions.

3.2 Other quasiprobability distribution functions

Wigner function is not the only useful quasiprobability distribution for the quantum harmonic oscillator. More in general, the normalized quasiprobability distribution associated to the density matrix ρ can be defined as the Fourier transform of the s -parametrized characteristic function $\chi(\xi, s)$ [37, 38]

$$W(\beta, s) = \int \frac{d^2\xi}{\pi} e^{\beta\xi^* - \beta^*\xi} \chi(\xi, s), \quad (16)$$

where

$$\chi(\xi, s) = \text{Tr}[\rho e^{\xi\hat{a}^\dagger - \xi^*\hat{a}} e^{\frac{1}{2}s|\xi|^2}]. \quad (17)$$

For $s = 0$ we obtain the Wigner function, $s = 1$, and -1 giving the P function and the Husimi Q function, respectively. These distribution functions correspond to symmetric, normal and antinormal ordering of the creation and annihilation operators, respectively.

The three distribution functions are closely related, and can be transformed into one another via a convolution relation. For $\tilde{s} < s'$, one has

$$\begin{aligned} W(\beta, \tilde{s}) &= W(\beta, s') \star G(s' - \tilde{s}, \beta) \\ &= \int d^2\theta W(\theta, s') G(s' - \tilde{s}, \beta - \theta), \end{aligned} \quad (18)$$

where

$$G(\kappa, \beta) = \frac{2}{\pi\kappa} \exp\left(-2 \frac{|\beta|^2}{\kappa}\right). \quad (19)$$

It is useful to note that the generalized distribution function of Eq. (16) is actually a continuous function of s , giving a continuum of different distribution functions, all of them obeying the relation of Eq.(18). This fact will be used later on, as it is the foundation of one of the definitions of nonclassicality I have studied, namely, the nonclassical depth, which is based on the amount of convolution the P function of the initial state can withstand until it is transformed into a Q function [39].

The effect of the convolution operation in Eq. (18) is to smooth out details of the s -parametrized distribution function. For example, while the P function can have severe singularities (of higher order than the delta function), in the Wigner function these are smoothed out. The Wigner function in turn can still take negative values but further convolving into a Q function damps the negativities so that the Q function is always a well-behaved, positive function. We will take advantage of this convolution property by connecting it to the dynamics of a particular non-classical state.

Having now defined the quasiprobability distributions, we can go back to the question of how to define non-classical states. Many different definitions based on the aforementioned distributions exist in the literature. Based on the convenient properties of the coherent state as the closest to a classical state, the original definition for nonclassicality was presented by Glauber and Sudarshan in 1963. According to this definition, a state is classical if it can be expressed as a statistical mixture of coherent states. This condition is equivalent to saying that the P function [37, 40–42] of the state is a positive, well-defined probability distribution [42]. The problem with this definition, from an experimental point of view, is that due to the strong singularities existing in the P function, measuring whether or not a given state is nonclassical is practically impossible using this criterion.

Many related measures and definitions for nonclassical states have been developed since [38, 39, 43–50], also for multimode fields [51–54]. Negativity of the Wigner function is another popular criterion used. However, due to convolution, some states that are nonclassical according to the P function definition, are not captured by the Wigner function formalism. The different approaches are not equivalent, so the complete characterization of nonclassical states, in particular a measurable criterion that is both necessary and sufficient, does not exist, except for pure states [45].

In paper IV we have used five different definitions of nonclassicality to study the transition process from quantum to classical. Putting emphasis on the physical meaning of each definition, I will present in the next chapter the problem, and the results obtained during my PhD studies.

4 Transition from quantum to classical

Quantum physics and classical physics deal with seemingly different size scales. The realm of atoms and photons is rich with quantum phenomena such as entanglement and superposition, whereas larger objects, like cats or dogs, can be adequately described by classical physics and do not routinely possess any quantum features.

This border has been previously taken as separation between qualitatively different realms, but recently the idea that there might not be a strict separation between the two has become dominant. Rather, the classical behavior is stemming from the quantum laws, decoherence induced by the environment mediating the emergence of classicality.

The apparent paradox arising from the application of quantum mechanics to macroscopic objects is famously illustrated by E. Schrödinger in his cat-in-the-box –thought experiment [55]. Consider a radioactive atom trapped in a box with alive cat. If the atom decays, it releases a mechanism that breaks a bottle of poison, killing the cat. If the atom does not decay, the cat lives. Now, if the quantum mechanical picture is valid, and one does not measure what is the state of the atom after some time, the statistics of radioactive decay process gives the following state of the cat–atom –system

$$|\Psi\rangle = \alpha|\text{atom decayed}\rangle|\text{cat dead}\rangle + \beta|\text{atom notdecayed}\rangle|\text{cat alive}\rangle. \quad (20)$$

The above equation essentially means that the cat, too, is in a superposition state of being both alive and dead. The thought of such macroscopic superpositions emerging from the entangling interaction between atom and cat contradicts our intuition. Moreover, such superpositions have never been observed for macroscopic objects like a cat. Although the double-slit experiment has been successfully performed with fullerene molecules, which are huge compared to electrons, they are still much smaller than cats. The precise process that ensures our everyday reality is not filled with weird superposition can not be said to have been conclusively understood, although many argue that the problem is merely philosophical.

4.1 Environment induced decoherence

If we accept the fact that macroscopic objects can not be in superposition states, we need a mechanism explaining what drives this change of behavior. Currently the prevailing explanation is environment induced decoherence (EID) [6,57]. EID mediates the so called quantum-to-classical transition, which

transforms non-local, entangled states (or superposition states for a single-mode case), into classically acceptable, local states by introducing preferred "pointer states" among all possible superpositions [56]. Classical reality is thus an emergent phenomenon of quantum theory.

In EID, the environment, which couples to all quantum systems, is seen to effectively monitor quantum superpositions, inducing a collapse to the corresponding statistical mixture of classical-like states (pointer states). In the context of Schrödinger cat in the thought experiment, the interaction with the environment would destroy the superposition, leaving the cat either dead or alive long before any measurement on the state of the atom or the cat takes place.

The passage from quantum to classical depends of course on the specific type of coupling to the environment. But if the coupling, and the initial state, is fixed, one more source of variation comes into play: how to tell apart the quantum from the classical? Here one can apply several definitions for nonclassicality. As we will see in the following, different definitions correspond to different ways in which the quantum to classical transition takes place. One way to monitor this transition is to follow the evolution of a quantum state analogous to the cat in the Schrödinger's thought experiment. In the next section I will describe in detail the model for the so called Schrödinger-cat state.

4.2 The life and death of the Schrödinger-cat state

With the name Schrödinger-cat state (or cat state, for short) I refer in the following to a quantum superposition of macroscopically or mesoscopically distinguishable states. In particular let us consider a quantum harmonic oscillator initially prepared in a superposition of coherent states with opposite phases,

$$|\Psi_{cat}\rangle = \frac{|\alpha\rangle + |-\alpha\rangle}{\sqrt{\mathcal{N}}} \quad (21)$$

where $|\alpha\rangle$ denotes a coherent state and

$$\mathcal{N} = 2[1 + \exp(-2|\alpha|^2)],$$

is the normalization constant. For the sake of simplicity we will assume the amplitude α real.

Coupling this initial state with a bosonic bath of oscillators at thermal equilibrium at temperature T causes decoherence that eventually leads to a

state that is a statistical mixture. If the reservoir spectrum is approximately flat, then the Markovian approximation holds.

Due to the Markovian approximation the master equation governing the evolution is a simplified version of Eq. (6). The decay coefficient γ is always positive and constant, and the master equation is in the Lindblad form,

$$\begin{aligned} \frac{d\rho(t)}{dt} = & \gamma(n+1)[2a\rho(t)a^\dagger - a^\dagger a\rho(t) - \rho(t)a^\dagger a] \\ & + \gamma n[2a^\dagger\rho(t)a - aa^\dagger\rho(t) - \rho(t)aa^\dagger]. \end{aligned} \quad (22)$$

Here n the mean occupation number of the thermal bath.

The quantum harmonic oscillator is an ideal model for studying the quantum-to-classical transition because it has both highly nonclassical and classical-like states. Monitoring the dynamics of the cat state (21) as it evolves into a statistical mixture according to Eq. (22) is a widely used method, which has been tested also experimentally [56]. Initially, the state is in a clearly nonclassical superposition state of two large amplitude coherent states. After EID, the state is a statistical mixture of coherent states. Remembering that the coherent state is the closest equivalent of a classical point in phase space, the final state can be considered classical.

Various definitions for nonclassicality can be applied to study the quantum-to-classical transition problem. The precise way of characterizing the transition leads to different dynamical features and interpretations. In the following I introduce five nonclassicality criteria which are then used to study analytically the time evolution of the cat state. These are the peak of the interference fringes of the Wigner function, the nonclassicality depth, the negativity of the Wigner function, Vogel nonclassicality criterion and the Klyshko criterion.

4.3 Time evolution of nonclassicality

Let us consider the five different nonclassicality criteria and apply them to the Schrödinger-cat state (21) evolving under the master equation (22). We are interested in finding if, after a finite time, the state is no longer nonclassical, according to each of the criteria. This time determines the threshold time for the quantum-to-classical transition.

4.3.1 Peak of the interference fringe

The traditional way to characterize the emergence of classicality is to use the interference term that appears in the Wigner function of the cat state [58–61],

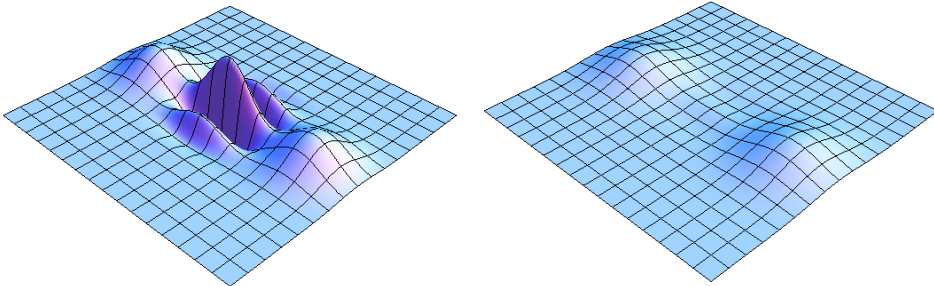


Figure 1: Schrödinger-cat state for amplitude $\alpha = 2$ at initial time (left) and after the state has decohered (right).

as can be seen from Fig. 1. These fringes oscillate obtaining also negative values. This deviation from a probability distribution is a sign of nonclassicality, and therefore the fringes are a natural object for studying the transition. Disappearance of the fringes means that, according to this definition, the state has become a mixture of coherent states, that is, classical, as in Fig. 1.

The fringes are quantified by the fringe visibility function [58], defined as

$$\begin{aligned}
 F(\alpha, t) &\equiv \exp(-A_{int}) \\
 &= \frac{1}{2} \frac{W_I(\beta, t)|_{\text{peak}}}{[W^{(+\alpha)}(\beta, t)|_{\text{peak}} W^{(-\alpha)}(\beta, t)|_{\text{peak}}]^{1/2}}, \quad (23)
 \end{aligned}$$

where $W_I(\beta, t)|_{\text{peak}}$ is the value of the Wigner function at $\beta = (0, 0)$ and $W^{(\pm\alpha)}(\beta, t)|_{\text{peak}}$ are the values of the Wigner function at $\beta = (\pm\alpha, 0)$, respectively.

The time evolution of the fringe visibility for an oscillator initially prepared in a cat state and then evolving in a Markovian damping channel, as the one described by Eq. (22), reads as follows [62]

$$F(\alpha, \tau) = \exp \left[-2\alpha^2 \left(1 - \frac{C_t^2}{1 + 2D_t} \right) \right], \quad (24)$$

where

$$C_t = e^{-\gamma t} \quad D_t = n(1 - e^{-2\gamma t}). \quad (25)$$

As we can see from Eq. (24) the emergence of classicality occurs asymptotically as the fringes are lost. The evolution of the fringe visibility has been monitored also experimentally with Schrödinger-cat states of light as a proof

of principle of the EID [59,61]. Similar experiments have been performed with trapped ion systems [60,63].

One problem with this definition is that no known operatorial expression can be given for the fringe visibility. That is, no known operator is directly connected to the fringe visibility function. Rather, it is based on the reconstruction of the Wigner function, which in turn requires full knowledge of the system state. In reality such full knowledge is usually difficult to obtain. Even with tomographic measuring techniques, the density matrix of the system can be reconstructed only within some confidence interval. Therefore the height of the interference peak is affected, in a nonlinear way, by the reconstruction technique [64].

4.3.2 Nonclassical depth

Nonclassical depth is a nonclassicality measure introduced by Lee [39], and later with a slightly different formalism by Lütkenhaus and Barnett [38]. The measure is based on the continuous quasiprobability distribution (16) and the related convolution relation in Eq. (18).

In short, given a density matrix of a quantum state, and the corresponding P function, the nonclassical depth is the answer to the following question: how much does the P function of the state need to be convoluted until it is a positive and regular function? In the formalism of Eq. (16), arriving to a Q function (i.e., $W(\beta, -1)$) guarantees the positivity and regularity. The nonclassical depth therefore uses any deviation from a classical probability distribution as a sign of nonclassicality.

The s -parametrized quasidistribution can be used to express other distribution functions as a convolution of the P function. By setting $s' = 1$, we get from Eq. (18)

$$W(\beta, s) = P(\beta) \star G(1 - s, \beta). \quad (26)$$

Now, the nonclassical depth is defined as

$$\eta = \frac{1}{2}(1 - \bar{s}), \quad (27)$$

where \bar{s} is the largest value of s for which $W(\beta, s)$ is positive.

Nonclassical depth is bounded from above. The maximum value, 1, is obtained by pure states other than a coherent state, for which $\eta = 0$, in accordance with the fact that it is the closest classical state [38]. Squeezed states have $0 \leq \eta \leq 1/2$, while mixed states can have any value of $\eta < 1$.

The usefulness of the nonclassical depth to the study of quantum-to-classical transition comes from the fact that the evolution of the cat state can be given in a similar form to Eq. (26). The solution to master equation (12) can be given in terms of the normally ordered (i.e., P function related) characteristic function $\chi(\xi, s = 1) \equiv \Phi(\xi)$. The time evolution of the characteristic function reads

$$\Phi_t(\xi) = \Phi_0(C_t \xi) \exp(-D_t |\xi|^2), \quad (28)$$

where the coefficients C_t and D_t are the same as in Eqs. (25) and Φ_0 is the characteristic function at time $t = 0$. By inserting this expression in Eq. (18) and choosing $s = 1$, we obtain the following Fourier transform relation:

$$P_t(C_t \beta) = \frac{1}{C_t^2} \int \frac{d^2 \xi}{\pi} \Phi_0(\xi) e^{-\frac{D_t}{C_t^2} |\xi|^2 + \beta \xi^* - \beta^* \xi}. \quad (29)$$

From the theory of Fourier transforms we know that the Fourier transform of a product of two functions is equal to the convolution of the two corresponding Fourier transforms. Equation (29) can therefore be recast in the form (see Eq. (26))

$$\begin{aligned} C_t^2 P_t(C_t \beta) &= P_0(\beta) \star G(1 - s_t, \beta) \\ &\equiv W(\beta, s_t), \end{aligned} \quad (30)$$

with

$$s_t = 1 - 2v_t, \quad v_t = D_t / C_t^2. \quad (31)$$

In words, the effect of the reservoir is to turn the P function of the initial state into a quasiprobability distribution function $W(\beta, s)$ of the initial state. This means that whenever $W(\beta, s)$ becomes positive, that is, when s reaches -1 so that W corresponds the Q function, the state has become classical in the sense that its P function is a proper probability distribution and therefore the state can be expressed as a statistical mixture of coherent states. The upper limit for the disappearance of nonclassicality is obtained from Eq. (31) by choosing $s_t = -1$. The corresponding time is

$$\tau_P = \frac{1}{2} \ln \left(\frac{1}{n} + 1 \right) = \frac{\hbar \omega}{2k_B T}, \quad (32)$$

where the result is given in units of the damping constant γ , i.e., $\tau_P = \gamma t_P$. Unlike the fringe visibility disappearance, here a finite time for the transition from quantum to classical is obtained (for high temperatures).

It is worth stressing that τ_P is indeed an upper bound to the nonclassical depth, and therefore to the quantum-to-classical transition time, for any initial nonclassical state since it corresponds to the time at which the P function of any initial state has evolved into a positive distribution function, i.e., the Q function, and since at all times $t > 0$ the evolved state is a mixed state. Thus, τ_P is independent of the cat state amplitude α . In the spirit of sudden death of entanglement since the quantumness of the state is lost in a finite time, we denote this upper limit τ as the sudden death time for the Schrödinger-cat state.

4.3.3 Negativity of the Wigner function

The third nonclassicality indicator here considered is the negativity of the Wigner function. It is a commonly used criterion largely due to the fact that homodyne detection allows the measurement of the Wigner function, whereas the P function can not be directly measured. However, it is well known that the Wigner function does not capture all the nonclassical states. Squeezed states are a prime example of this fact.

Tracking the dynamics of the negativity of the Wigner function becomes easy to handle when we apply the same line of reasoning as in the case of the nonclassical depth. We saw before that the dissipative dynamics transforms the initial P function into a Q function, but it is easy to see that, before that, the initial P function becomes the Wigner function (see Eq. (18)). The evolution of the negativity of the Wigner function can be obtained from Eq. (29). It is straightforward to derive the upper limit to the disappearance of negativity of the Wigner function by choosing $s = 0$ in Eq. (31). In this way we obtain

$$\tau_W = \gamma t_W = \frac{1}{2} \ln \left(\frac{1}{2n} + 1 \right). \quad (33)$$

We conclude that the negativity of the Wigner function is lost faster than nonclassicality according to nonclassical depth, since for high T -reservoirs, i.e., for $n \gg 1$, $\tau_W \approx 1/8n$ and $\tau_P \approx 1/4n = 2\tau_W$.

4.3.4 Vogel criterion

The P function criterion for nonclassicality is perhaps the most fundamental, but experimentally difficult due to the possible strong singularity of the P function. In the year 2000, W. Vogel introduced a criterion equivalent to the P function criterion, while at the same time being experimentally accessible.

The key idea behind Vogel criterion for nonclassicality was that there existed a direct relation between a well-behaved P function and a well-behaved noise-subtracted quadrature distribution [44]. Since quadrature distributions are experimentally measurable, the classicality of the P function can be evaluated in a reliable way using this connection.

It was later pointed out by L. Diósi that some nonclassical states were not captured by the criterion [65]. This led to a generalization of the original proposal. The new complete criterion is actually a hierarchy of criteria, the original definition being the first order in this set of criteria. This infinite set of inequalities allows, in principle, to characterize all nonclassical states (according to the P function nonclassicality) by simple measurements overcoming the problem of high order singularities in P [45].

In principle, however, if the first order inequalities are satisfied one should still check till an arbitrary n th order. In practice, the situation is not so severe. Until now, the only example of a nonclassical state not captured by the first order criterion is the one suggested by Diósi. For a multitude of nonclassical states, the Vogel first order criterion works well. The (first order) Vogel criterion can be formulated in the following way: the state is nonclassical if there exists values u and v such that

$$|\Phi(\xi)| > 1 \tag{34}$$

for the normally ordered characteristic function Φ , where $\xi = u + iv$. This criterion is intuitive in the sense that the P function related characteristic function is normalized to unity. If the absolute value exceeds one at some point, it needs to become negative at some other point, corresponding to a nonclassical state.

The symmetrically ordered characteristic function can be measured directly with balanced homodyne detection. Formulating the first order criterion in terms of the symmetrically ordered characteristic function χ we obtain

$$|\chi(\xi, 0)| > \chi_0(\xi, 0) \equiv \exp\left(-\frac{1}{2}|\xi|^2\right) \tag{35}$$

where $\chi_0(\xi, 0)$ is the characteristic function of the ground state of the system oscillator [44]. Formulating a criterion for nonclassicality in terms of the inequality (35) essentially means that complete state tomography is not anymore necessary to characterize the nonclassical status of a state. A single measurement satisfying inequality (35) is sufficient to detect nonclassicality, and maintaining a stable relation between the local oscillator and the optical

state becomes unnecessary [66]. This makes checking for the nonclassicality of a state much simpler compared to full state tomography.

The two conditions in Eqs. (34) and (35) are completely equivalent, and can be obtained from one another via the transformation rule for the different characteristic functions. In this respect, it does not matter which one of the criteria is used to study the quantum-to-classical transition.

For our initial cat state of Eq. (21) the time evolution of the normally ordered characteristic function reads [67]

$$\Phi_t(u, v) = \frac{2}{\mathcal{N}} e^{-D_t(u^2+v^2)} \left[\cos(2C_t\alpha v) + e^{-2\alpha^2} \cosh(2C_t\alpha u) \right], \quad (36)$$

where C_t and D_t are given in Eq. (25).

Numerical evaluation of this quantity to determine when it becomes less than one tells us when the initially nonclassical cat state becomes classical. In light of the discovery by Diósi of a nonclassical state not captured by this criterion, and the resulting bigger set of conditions, one might argue that the condition (36) is not sufficient to determine whether the state has really become classical. However, our argument was that since the initial, nonclassical cat state clearly is nonclassical according to Vogel's first order criterion, and during the evolution ceases to be nonclassical according to the definition in question, the state clearly loses some, crucially quantum property it initially had. The choice we have made, is to associate the first order criterion to the quantum-to-classical transition. The transition takes place at time τ_V indicated by a dashed line in Fig. 2.

Since $\Phi_t(u, v) \leq \Phi_t(u, 0)$, in Fig. 2 we have plotted the contour line corresponding to $\Phi_t(u, 0) = 1$. According to the Vogel criterion in Eq. (34), after τ_V there exist no parameter value u for which the state would be nonclassical. Hence τ_V is the sudden death time of nonclassicality according to the Vogel nonclassicality criterion.

We have also evaluated the transition time as a function of the size of the cat state, that is, of the amplitude α . Unlike in the fringe visibility criterion, with the Vogel criterion an increase in the initial separation corresponds to a longer time before the state becomes classical. According to our numerical study the transition times as a function of α seem to saturate, possibly indicating an upper bound for the onset of classicality for initially highly nonclassical states. In fact, analytically setting $\alpha \rightarrow \infty$ it is possible to obtain the following necessary and sufficient condition for the state to be classical

$$C_t^2 \leq 2D_t. \quad (37)$$

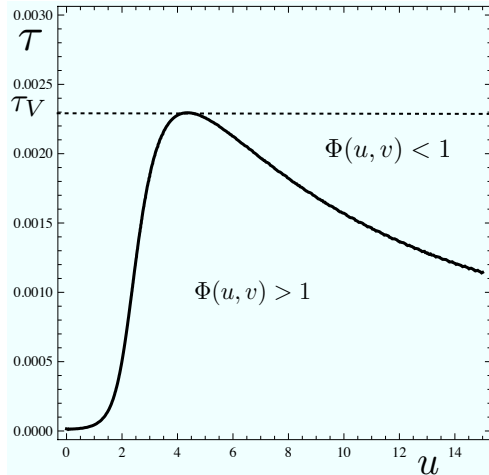


Figure 2: Vogel nonclassicality condition as a function of $\tau = \gamma t$ and u , for $v = 0$, $n = 100$ and $\alpha = 2$. The solid line corresponds to $\Phi_t(u, 0) = 1$. The state is nonclassical in the area under the curve. The time τ_V is the time at which the state becomes classical.

It is noteworthy that Eq. (37) coincides with the equation defining the sudden death time τ_W in terms of the negativity of the Wigner function. Hence,

$$\tau_V(\alpha) \xrightarrow{\alpha \rightarrow \infty} \frac{1}{2} \ln \left(1 + \frac{1}{4n} \right) \equiv \tau_W. \quad (38)$$

4.3.5 Klyshko criterion

The final criterion deals with photon number probabilities, making it experimentally accessible. In 1996, D. N. Klyshko showed that an equivalence between a phase-averaged P function,

$$F(r) = \int_0^{2\pi} \frac{d\phi}{2\pi} P(re^{i\phi}), \quad (39)$$

and an infinite set of inequalities concerning photon number probabilities $p(m) = \langle m | \rho | m \rangle$ exists [43]. These inequalities give a necessary and sufficient condition for nonclassicality in terms of the negativity of $F(r)$ [43]. The simplest sufficient criterion for nonclassicality takes the form [43, 68]

$$B(m) \equiv (m+2)p(m)p(m+2) - (m+1)[p(m+1)]^2 < 0. \quad (40)$$

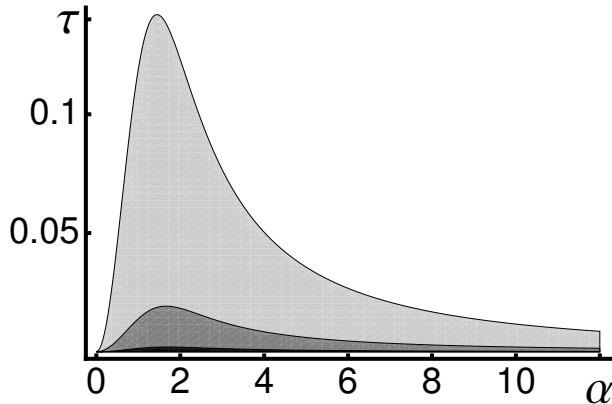


Figure 3: The nonclassicality condition $B(1) < 0$ is satisfied in the gray areas of the plot showing the transition time from quantum to classical as a function of the initial wave packet separation. Here $\tau = \gamma t$, and (from larger to smaller areas) $n = 1, 10, 100$. The border of each gray area individuates the function $\tau_K(\alpha)$, i.e., the sudden death time according to Klyshko criterion.

For $F(r)$ to be negative, it is sufficient that this condition is satisfied by just one non-negative integer number m .

The photon number probabilities can be obtained from

$$p(m, t) = \frac{1}{\pi} \int du dv \Phi_t(u, v) \chi_m(u, v), \quad (41)$$

where $\Phi_t(u, v)$ is the characteristic function of the (evolved) cat state from Eq. (36) and $\chi_m(u, v) = \exp(-u^2 - v^2) L_m(u^2 + v^2)$ is the anti-normally ordered characteristic function of the Fock number state $|m\rangle$, $L_m(x)$ being the m -th Laguerre polynomials. For our initial cat state, the simplest condition showing the nonclassicality is provided by negativity of $B(1)$.

Nonclassicality condition $B(1) < 0$ is plotted in Fig. 3 for different reservoir temperatures. An interesting detail is the fact that there exists a preferred value for the initial separation, $\alpha \approx 2$, for which nonclassicality is sustained for the longest period of time. This would imply that certain arbitrary cat states are more favorable when fighting decoherence. In truth, this behavior has to do with the structure of $B(1)$, which is composed of an overlap of the cat state characteristic function and the characteristic function of Fock states with small mean occupation numbers m . This consideration, together with the

fact that higher order $B(m)$ -nonclassicality conditions seem to be subsumed by $B(1) < 0$, have led us to conclude that the Klyshko criterion is not suitable to follow the time evolution of nonclassicality for highly separated superpositions. For smaller separation, however, this method has clear experimental advantage, since photon number distributions may be effectively reconstructed [69,70] and in some cases also directly measured [71,72].

4.4 Emergence of classicality

In the previous subsections I have summarized the results we obtained in paper IV. Our aim was not to give a precise characterization of the amount of nonclassicality available in the evolving cat-state at every instant of time. Rather, we wanted to obtain qualitative knowledge on the time instant, if a finite time exists, where nonclassicality associated to the cat state vanishes. This maximum time for the preservation of nonclassicality is the threshold time for the emergence of classicality in the quantum-to-classical transition. The results are summarized in Table 1.

The only qualitatively different nonclassicality definition is the fringe visibility function which does not give a finite transition time for the state to become classical. Instead the state evolves asymptotically towards classicality. For all other measures of nonclassicality, there exist a finite time after which the evolved state ceases to be nonclassical according to the corresponding criterion. We call this threshold time τ the "death-time for the Schrödinger cat-state".

The fringe visibility, although widely used, suffers from the lack of any known operatorial interpretation. The Vogel criterion, on the other hand can be measured for freely propagating radiation modes, cavity-field modes [73] and the quantized center-of-mass motion of a trapped ion in harmonic potential [74]. This last method offers an operatorial approach to the nonclassicality problem. It was shown in [74] that the full state information of a vibrational motion of a trapped ion can be obtained simply by monitoring the evolution of the ground state occupation probability in a long-living electronic transition. This gives a clear connection between the transition from quantum to classical and the ground state probability.

The transition times τ vary for all the nonclassicality criteria. The Klyshko criterion is the most sensitive, while the nonclassical depth, which is identical to the P function being a proper probability distribution, is the most robust against the emergence of classicality. However, the nonclassical depth is not directly measurable. Negativity of the Wigner function gives the next longest

time for the persistence of nonclassicality. This quantity can be approximately evaluated via homodyne detection. Moreover, it has been recently shown, that measuring merely two conjugate variables, instead of performing full state tomography, is sufficient to observe the negativity of the Wigner function in a certified, error-free way [75].

The Vogel criterion gives only slightly shorter transition time than the negativity of the Wigner function. The full set of conditions, and not just the first order condition, would give a transition time equal to the nonclassical depth / negativity of the P function. As we have pointed out, however, the full set of criteria is impossible to tackle experimentally. The strength of the Vogel (first order) criterion lies in the fact that it is very simple, and has a direct correspondence with a physical quantity, as described above. Although it does not capture all nonclassical states, we conclude that since this criterion is satisfied for the initial cat states, it singles out a property that belongs to such superpositions. It is therefore meaningful to state that the finite-time quantum-to-classical transition of the cat state coincides with the time at which the nonclassicality property of Vogel's first order criterion is lost.

Our result is conceptually interesting from the point of view of decoherence and entanglement. Entanglement is under certain conditions known to disappear completely in a finite time, a phenomenon known as entanglement sudden death [76]. Nonclassicality is a prerequisite to entanglement in continuous variables systems. While the coherences indeed disappear only asymptotically, we have demonstrated that under many nonclassicality definitions, the loss of nonclassicality can occur at a finite time, bridging the conceptual gap between entanglement and decoherence.

Table 1: Threshold time for quantum-to-classical transition (death of the cat) according to different indicators of nonclassicality for $\alpha = 2$ and $n = 50$. The last column summarizes the dependence of the threshold value on the cat amplitude.

Nonclassicality measure	threshold time τ	dependence on α
Klyshko criterion	0.0019	τ is maximum for $\alpha \approx 2$
Vogel criterion	0.0023	saturates with growing α
Negativity of $W(\beta)$	0.0025	independent of α
Negativity of $P(\beta)$	0.0050	independent of α
Fringe visibility	∞	proportional to α^2

5 Structured reservoirs and reservoir memory

The second part of my Thesis focuses on non-Markovian effects stemming from the coupling to a reservoir with structure. Structured reservoirs are reservoirs for which the coupling between each reservoir mode and the system shows strong variations. As such they induce more complicated dynamics than reservoir with approximately flat spectra. For example they may induce back-flow of information and/or energy from the reservoir into the system. In the next section I will describe several examples of non-Markovian dynamics, induced by different reservoir structures.

5.1 Non-Markovian dynamics

Non-Markovianity has been studied, starting from its very definition extensively over the past decade [14,15,77]. A key characteristic of non-Markovianity is the memory effects causing, for example, re-coherence when information that has been lost into the environment partly flows back into the system. Information flow has even been formulated as a measure of non-Markovianity in a recent paper by H.-P. Breuer *et al.* [78], and extended to continuous variable systems in [13].

In some cases non-Markovian memory effects are directly connected to situations for which the past history of the system affects its future dynamics. Phenomenological memory kernel master equations carry the memory in a memory kernel integral, but the existence of exact master equations has shown that explicit dependence on past history is not required for the non-Markovian effects to occur. In time-local master equations, characterized by time-dependent decay rates, the back-flow of information is often related to negativity of the decay rates [12]. In general, one can say that Lindblad-type master equations with always positive (even if time-dependent) decay rates lead to Markovian dynamics.

Non-Markovianity often arises from the short-time correlations between the system and the reservoir. Markovian dynamics are always the result of approximations, whereas the exact dynamics is always non-Markovian. For weak couplings, generally non-Markovian effects dominate the dynamics at short time scales, typically determined by the cutoff frequency ω_c of the spectrum. Non-Markovian effects occur in time scales characterized by the condition $\omega_c t \leq 1$.

System-reservoir correlations are usually significant and can not be neglected if the reservoir spectrum is highly structured. We have examined the latter case, where the reservoir has a structure. In the next section I will

present the class of environmental spectra which I have considered in papers I-III.

5.2 Structured reservoirs

The reservoir spectra we have used are known as Ohmic spectral densities

$$J(\omega) = g^2 \omega_c^{1-s} \omega^s e^{-\omega/\omega_c}. \quad (42)$$

The exponential cutoff term is introduced to eliminate divergencies in the $\omega \rightarrow \infty$ limit, ω_c is the cutoff frequency, g is a dimensionless coupling constant we assume small to satisfy the weak coupling approximation and s is a parameter characterizing the type of the spectrum. The parameter s can take values < 1 , 1 or > 1 , corresponding to the so called sub-Ohmic, Ohmic, and super-Ohmic spectral densities. We consider some exemplary spectra corresponding to values of s equal to $1/2$, 1 and 3 .

The spectral distribution

$$I(\omega) = J(\omega) \left[N(\omega) + \frac{1}{2} \right], \quad (43)$$

where $N(\omega)$ is the same as in Eq. (13), contains also information about the occupancy of each mode. The spectral distribution depends on the temperature of the reservoir through the average number of reservoir thermal excitations, $N(\omega)$. At high temperatures T , $N(\omega) \approx k_B T / \omega$, while for zero temperature $N(\omega) = 0$. I will focus on these two temperature regimes.

The dynamics of the system are governed by yet another key parameter, the so-called resonance parameter, defined as the ratio between the cutoff frequency and the system oscillator frequency ω_0 ,

$$r = \frac{\omega_c}{\omega_0}. \quad (44)$$

Changes in this parameter correspond to shifting the system oscillator frequency with respect to the reservoir spectrum. Since the spectrum has a frequency dependent structure, changing the resonance parameter affects the effective coupling between the system and the environment. The resonance parameter can be manipulated experimentally, allowing control over the system-reservoir coupling [63, 79].

Changing the parameter r also affects directly the validity of the secular approximation. Since ω_0 and ω_c are connected via the definition of the resonance parameter, fixing r places the following constraint with respect to secular

approximation. For $r \gg 1$ we have $\omega_c \gg \omega_0$. Under this condition making the secular approximation is not consistent with following the non-Markovian dynamics, because secular approximation amounts to coarse graining over times scales of the order of $1/\omega_0$, while non-Markovian effects are visible for $\omega_c t \leq 1$.

With these reservoir parameters we will tackle the dynamics of non-Markovian dissipation and squeezing in the next Chapter.

6 Decoherence and dissipation under different reservoirs

In the first part of the Thesis I have examined decoherence as a welcomed mechanism for the transition from quantum to classical. In the rest of the Thesis, the point of view is centered more on the harmful effects decoherence and dissipation have on quantum technologies.

Quantum computation relies its functionality on the properties of artificially produced quantum states [35]. The unavoidable coupling to the environment, however, very quickly destroys the desired properties by the mechanisms of decoherence and dissipation. Building a working quantum computer is still a distant goal, but many proof-of-principle experiments and components that could eventually be utilized in a quantum computer have already been tested in the laboratories [80–83].

Different quantum technologies, such as quantum cryptography, quantum metrology and quantum logic gates, can be implemented in a variety of ways. Qubits, the quantum bits that act as the quantum mechanical counterparts of ordinary bits of computation, can be prepared with optical states of light [84,85], nuclear spins [86], trapped ions [87], cavity QED or solid state devices, such as very narrowly spaced Josephson junctions on a chip [88] or coupled quantum dots. All these qubit implementations are by construct, surrounded by different types of environmental modes. Understanding decoherence and dissipation for different types of environments is therefore necessary.

Quantum mechanical systems can also be used very effectively to simulate other, more complicated quantum systems [89]. It has been shown very recently, in the trapped ions context, that open quantum systems are also amenable to quantum simulation [90]. Considering the difficulties faced in solving most open quantum system master equations, simulating them effectively would be very useful to test fundamental models of open system dynamics. Quantum simulations, too, are vulnerable to decohering effects, while requiring a certain time to run the simulation. On-going theoretical and experimental investigation is devoted to the quantum state deteriorating effects of the environment. Our work is located within this framework, elucidating the central role played by the spectral structure of the environment.

6.1 Solution for the equation of motion

For the purpose of examining the decay dynamics of the quantum Brownian motion model, we need to solve the master equation. In our case, the so-

lution can be obtained analytically under the weak coupling approximation. This is very useful for the interpretation of our results, because it allows us to gain knowledge on the connection between different reservoir spectra, and the corresponding decay dynamics. Both the exact and the weak coupling approximated master equations have the same operatorial form of solution, with different time-dependent coefficients. For studying the dissipation we can use the secular approximated master equation of Eq. (12) for all values of the resonance parameter because the quantity we examine, the heating function, belongs to a class of observables not affected by the secular approximation [10].

The solution of the master equation (12), obtained through algebraic properties of superoperators, reads [10]

$$\chi_t(\xi) = e^{-\Delta_\Gamma(t)|\xi|^2} \chi_0[e^{\Gamma(t)/2} e^{-i\omega_0 t} \xi], \quad (45)$$

where χ_0 is the initial quantum characteristic function, and the coefficients take the form

$$\Gamma(t) = 2 \int_0^t \gamma(t_1) dt_1, \quad (46)$$

$$\Delta_\Gamma(t) = e^{-\Gamma(t)} \int_0^t e^{\Gamma(t_1)} \Delta(t_1) dt_1, \quad (47)$$

where $\Delta(t)$ and $\gamma(t)$ are diffusion and dissipation terms, given in Eq. (13).

6.2 Decay channels

The front factors of the master equation (12), $[\Delta(t)+\gamma(t)]/2$ and $[\Delta(t)-\gamma(t)]/2$, consisting of the diffusion and dissipation terms are the relaxation rates for the two decay channels that exchange energy and information between the system and the reservoir. In the Fock state basis they represent the emission and absorption of one quantum of energy, that is, $[\Delta(t) + \gamma(t)]/2$ is the rate associated to the cooling down process, for which one quantum of energy is transferred from the system to the reservoir ($|n\rangle \rightarrow |n-1\rangle$), while $[\Delta(t)-\gamma(t)]/2$ describes the absorption rate of one excitation from the reservoir ($|n\rangle \rightarrow |n+1\rangle$). Correspondingly, we will denote these channels as the (transition) down and up channels.

These transitions that describe the heating and cooling of the quantum harmonic oscillator destroy the quantum coherence of initial superpositions. We have obtained analytical expressions for the decay rates for both high- T and zero- T reservoirs. For high temperatures, one can see that $\Delta(t) \gg \gamma(t)$,

and the decay down and up channels operate, for times much shorter than thermalization time, at approximately same rate, $\Delta(t)/2$.

From these analytical results we are able to show that $\Delta(t)$ oscillates taking temporarily negative values for $r \ll 1$ for all reservoir types here considered. The origin of these oscillations can be traced back to the form of the environment. Indeed, for $r \ll 1$, large portion of the spectrum is located in the low frequencies, that is in the region $\omega < \omega_0$.

For zero- T reservoir, both channels $[\Delta(t) + \gamma(t)]/2$ and $[\Delta(t) - \gamma(t)]/2$ oscillate for $r \ll 1$. In addition, the oscillations persist even for $r = 1$, unlike in the high- T case. For the super-Ohmic reservoir, a strong initial jolt is visible in the decay rates for all resonance parameter values. We have identified the origin of this strong initial jolt. It is present when the peak of the spectrum lies in the frequency region $\omega > \omega_c$.

6.3 Non-Markovian energy transfer

Dissipation is the energy transfer between the system and the reservoir. Under non-Markovian dynamics there may appear oscillations in the dynamics of the mean energy of the system, indicating that the flow of energy is temporarily reversed, as we will now see. The heating function, which is proportional to the mean energy of the system, is defined as

$$\langle n \rangle = \langle a^\dagger a \rangle. \quad (48)$$

The analytical expression for the heating function can be easily obtained from the characteristic function solution of the master equation. It reads

$$\langle n(t) \rangle = e^{-\Gamma(t)} \langle n(0) \rangle + \frac{1}{2} \left[e^{-\Gamma(t)} - 1 \right] + \Delta_\Gamma(t), \quad (49)$$

where $\Gamma(t)$ and $\Delta_\Gamma(t)$ are defined in Eq. (47). Non-Markovian dynamics manifest for short time scales. Therefore we can assume that the time scales of interest are much shorter than the thermalization time, t_{th} . The expression for the heating function is thus simplified to

$$\langle n(t) \rangle = \int_0^t [\Delta(t_1) - \gamma(t_1)] dt_1. \quad (50)$$

For high temperature reservoirs, $\Delta(t) \gg \gamma(t)$, allowing a further simplification of the heating function,

$$\langle n(t) \rangle \approx \int_0^t \Delta(t_1) dt_1. \quad (51)$$

Through $\Delta(t)$ and $\gamma(t)$, the heating function is a function of the reservoir spectral density. The analytic expressions for the decay rates allow us to obtain analytically the dynamics of the energy transfer occurring at short time scales, and obtain information on the precise way changes in the reservoir spectrum affect the heating function.

The heating function dynamics can be divided into two types of behavior. As a sign of non-Markovianity, the heating function oscillates for certain reservoir and resonance parameter values. These coincide with the values that produce negativities in the decay rates, as described above. Another feature in the dynamics is the monotonic growth, that dominates after the oscillations have ceased. Our main conclusion is that, for all three reservoir types, oscillations in the heating function originate from the low frequency part of the spectrum, while monotonic heating is caused by the resonant part of the spectrum, namely the value $I(\omega_0)$. For the case of Ohmic reservoir, a similar result already existed [91]. We have extended the result for a wider class of spectra.

The qualitative difference between high and low temperatures, according to our results, is that for the zero temperature reservoirs, oscillations both in the decay rates $\Delta(t)$ and $\gamma(t)$, and in the heating function n , persist for larger values of the resonance parameter. This is in agreement with the behavior of the decay rates.

6.4 Markovian limit and thermalization dynamics

Our results for the non-Markovian dissipation dynamics can be extended also to longer time scales simply by letting $t \rightarrow \infty$ in the integral of Eq. (13). After a certain reservoir-dependent time the constant, positive Markovian decay rates

$$\Delta_M = \pi I(\omega_0), \quad (52)$$

$$\gamma_M = \frac{\pi}{2} J(\omega_0), \quad (53)$$

are reached.

Inserting these expressions to the equation of the heating function (49) we get the evolution of the heating function for time scales up to thermalization,

$$\langle n(t) \rangle_M = N(\omega_0) (1 - e^{-\Gamma t}), \quad (54)$$

where $\Gamma = 2\gamma_M = \pi J(\omega_0)$. From this expression, we can express the reservoir thermalization time, in units of ω_0 , as follows

$$t_{th} = \omega_0/\Gamma = (\pi g^2)^{-1} r^{s-1} e^{1/r}, \quad (55)$$

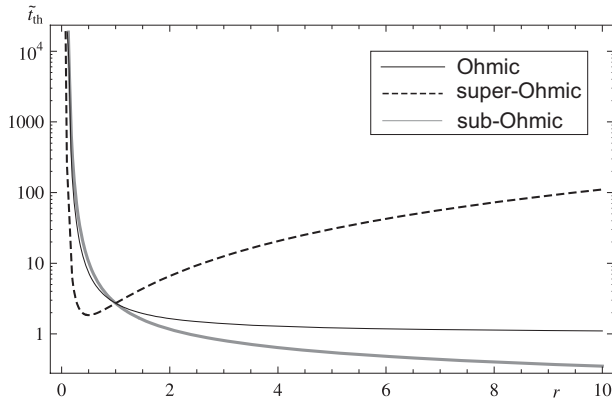


Figure 4: Thermalization times for different reservoirs. Here $\tilde{t}_{th} = \pi g^2 t_{th}$.

where r is defined in Eq. (44), s is given right after Eq. (42) and g is the dimensionless coupling constant. From Fig. 4 we see clearly how differently the different reservoirs affect even the thermalization dynamics of the system. In particular with the super-Ohmic reservoir increasing the value of r will, after $r \approx 0.5$, result in longer and longer thermalization times, allowing experimental control over the thermalization dynamics.

6.5 Decoherence

Decoherence process corresponds to the loss of coherences that are represented by the off-diagonal terms of the density matrix. Decoherence is dependent on the diffusion rate $\Delta(t)$, so its effectiveness can be traced back to the dynamics of this coefficient. Negative regions in the diffusion coefficient can sometimes cause recoherence, temporarily reversing the decoherence process. This was known to happen in qubit systems, but not for the decoherence process of a Schrödinger-cat state for continuous variable systems, as we will see in more detail in Chapter 7. It has been shown also, for qubit systems, that during the periods of negative decay rates, the system experiences quantum jumps that restore the quantum state before the jump had occurred. [22, 23].

It seems very intuitive that these effects, stemming from the non-Markovian dynamics, could be used as a tool to fight the harmful effects of decoherence, even in the continuous variable case. In theory this is indeed possible. We will examine decoherence more closely from the point of view of decoherence

control in Chapter 7, using the framework described in this and in the previous section.

First, let us take a closer look to another highly nonclassical feature also affected by the structured coupling, the squeezing.

6.6 Non-Markovian squeezing

The Heisenberg uncertainty principle for the variances of the dimensionless quadratures x and y states that $(\Delta x)^2(\Delta y)^2 \geq 1/4$. Squeezed states are the ones where the variance of one quadrature is smaller than that of the vacuum, that is, $1/4$ [92]. The other quadrature will have a larger variance in order not to violate the uncertainty principle. Squeezed states are quantum states with no classical analog since the uncertainty relation has no correspondence in classical physics. Under structured reservoirs, the degree of squeezing of a coherent state experiences environment induced effects that (depending on the parameters) may result in oscillations between the state being squeezed and not being squeezed.

Squeezed states are obtained by squeezing with a squeezing operator $S = \exp(1/2(za^2 - z^*a^{\dagger 2}))$, where $z = se^{-i\phi}$ is the squeezing parameter, and then displacing with the displacement operator $D = \exp(\beta_0 a^\dagger - \beta_0^* a)$ the vacuum state. To follow the dynamics of an initial squeezed coherent state,

$$|\beta_0, z\rangle = \hat{D}(\beta_0)\hat{S}(z)|0\rangle, \quad (56)$$

we use again the secularly approximated master equation (12). The non-Markovian dynamics of squeezed states are generally affected by the secular approximation, unlike the heating function. However, if we retain our analysis on the high temperature, weak coupling scenario, and focus only on the case where $r \ll 1$, the secular approximation is consistent with the non-Markovian time scales. [31].

The Wigner function, which we have already discussed in Ch. 3, gives a very useful representation of the squeezed states, as the distribution is literally squeezed along the axis defined by the squeezing angle. The Wigner function evolution can be obtained from the solution in terms of the quantum characteristic function in Eq. (45) simply by making a Fourier transform. With the help of the initial quantum characteristic function of the initial state, expressed as

$$\chi_0(\xi) = \exp\left[-\frac{1}{2}|\xi C_s - \xi^* e^{-i\phi} S_s|^2 + i(\xi^* \beta_0^* + \xi \beta_0)\right], \quad (57)$$

where $C_s = \cosh(s)$ and $S_s = \sinh(s)$, we obtain the following expression for the Wigner function:

$$W_t(\beta) = M \exp \left[\frac{-\beta_x^2}{(\Delta x)^2(t)} + \frac{-\beta_y^2}{(\Delta y)^2(t)} \right], \quad (58)$$

where we have assumed an initially squeezed and displaced vacuum state ($\beta_0 = 0$) with squeezing angle $\phi = 0$, and where

$$(\Delta x)^2(t) = \Delta_\Gamma(t) + \frac{e^{-\Gamma(t)}e^{-2s}}{2} \quad (59)$$

$$(\Delta y)^2(t) = \Delta_\Gamma(t) + \frac{e^{-\Gamma(t)}e^{2s}}{2} \quad (60)$$

are the variances of the dimensionless quadratures $x = (a + a^\dagger)/\sqrt{2}$ and $y = -i(a - a^\dagger)/\sqrt{2}$, with M a time-dependent normalization constant, and β_x and β_y are the real and imaginary parts of β [93, 94].

Focusing on the x -quadrature, the squeezing condition is $(\Delta x)^2 < 0.5$. If the variance is larger than this threshold value, the state is not squeezed. I have found that for the parameters used (high- T , $r \ll 1$) Ohmic and sub-Ohmic reservoirs induce more pronounced oscillations between the state being squeezed and not squeezed. The parameters affecting the dynamics are the reservoir type, the temperature and the initial squeezing. The reservoir type is mostly responsible for the shape of the curve describing the squeezing dynamics, while the temperature and the initial squeezing s simply shift the curve in the y -direction, i.e., with respect to the squeezing–non-squeezing border ($(\Delta x)^2 = 0.5$).

The dynamics of the quadrature follow the behavior of the decay rates $\Delta(t)$ and $\gamma(t)$. Based on the previous results, we can say that squeezing oscillations are present when the spectral distribution $I(\omega)$ is strongly peaked in the low-frequency regime $\omega < \omega_0$.

7 Decoherence control

Methods to control decoherence, and in particular to reduce its deteriorating effects on quantum systems are highly desired in the quantum information community. Decoherence is indeed a major obstacle in the realization of quantum devices. However, many schemes to fight against decoherence exist in the literature, ranging from decoherence free subspaces [95], quantum Zeno-control based strategies [96] to dynamical decoupling [97]. We have considered two possible mechanisms that could be used to control the decoherence dynamics of the system by means of reservoir engineering, or by manipulating the system–reservoir coupling in such a way that the decoherence rate is altered. Let us consider first the reservoir engineering scheme.

7.1 Reservoir engineering

Experiments dealing with artificial, engineered reservoirs, are rapidly developing. Currently reservoir engineering has been demonstrated in optical and microwave cavities [98–101], photonic crystals [102], ranging from controllable Ohmic environments [63, 79] to sub-Ohmic and super-Ohmic reservoirs [103]. The ability to modify in a controlled way the coherence properties and the decoherence rate of the system by acting on its environment, and in particular by modifying its spectral properties, is an interesting prospect from both theoretical point of view and in connection with the desire to create decoherence-free quantum systems for applicative purposes.

Non-Markovian theory is crucial in this task, since the structured reservoirs are characterized by non-negligible memory effects. In our work we have demonstrated in which way the decoherence rate of a Schrödinger-cat state (Eq. (21)) is affected by the type of the reservoir (Ohmic, sub-Ohmic or super-Ohmic), and by the resonance parameter in Eq. (44). Our analytical results shed light on the reservoir-dependent dynamics of decoherence, and on the role of modifying the resonance parameter.

As a signature for the decoherence process of the initial cat-state, we have used the fringe visibility function from Eq. (23). Our main goal in comparing the reservoir parameters, is to find the optimal conditions leading to the slowest environment induced decoherence.

The non-Markovian fringe visibility for $r \ll 1$ reads

$$F(\alpha, t) = \exp \left[-2\alpha^2 \left(1 - \frac{e^{-\Gamma(t)}}{2n(t) + 1} \right) \right], \quad (61)$$

where

$$n(t) = \int_0^t dt' \Delta(t'), \quad (62)$$

$$\Gamma(t) = 2 \int_0^t dt' \gamma(t'), \quad (63)$$

while in the opposite regime, $r \gg 1$, the function takes the form

$$F(\alpha, t) = \exp \left[-2\alpha^2 \left(1 - \frac{e^{-\Gamma(t)}}{4n(t) + 1} \right) \right]. \quad (64)$$

There is a factor of two difference in front of the heating function, $n(t)$, in the denominator. This means essentially that the $r \gg 1$ regime corresponds to an effective reservoir having twice the temperature T compared to the off-resonant regime. As discussed before in Section 5.2, we can not in general make a secular approximation in the $r \gg 1$ regime, since it would contradict the non-Markovianity assumption. Due to this, two extra terms in master equation (6) corresponding to two additional decay channels, are responsible for effectively faster decoherence process in the off-resonant case. Also, for $r \gg 1$, the effective coupling given by $I(\omega_0)$ is larger, resulting in faster decoherence.

For times $t \ll t_{th}$ the exponential factor $e^{-\Gamma t}$ is approximately one. The decoherence process is therefore only dependent on the heating function, which is a function of $\Delta(t)$. Unlike the heating function, the fringe visibility characterizing decoherence shows a similar, monotonic behavior for all three reservoir types (see Fig. 5). No recoherence takes place, even for times when $\Delta(t)$ is negative.

For both $r \gg 2$ and $r \ll 1$ the Ohmic reservoir induces the slowest decoherence, while the super-Ohmic and sub-Ohmic reservoirs decay in a very similar manner, both faster than the Ohmic case. From these two regimes, $r \gg 1$ induced much faster decoherence due to the fact that the effective coupling to the reservoir is stronger.

In the inset of Fig. 5 we show a comparison between the Markovian and non-Markovian initial dynamics. In the off-resonant case the non-Markovian decoherence takes place much faster than the Markovian one. This is due to the initial jolt in $\Delta(t)$ that is contributing to the very fast initial decoherence rate. For the $r \gg 1$ case, the Markovian decoherence is faster.

Decoherence control can be obtained if one is able to modify the natural reservoir spectrum into an Ohmic form. Then decoherence would slow down

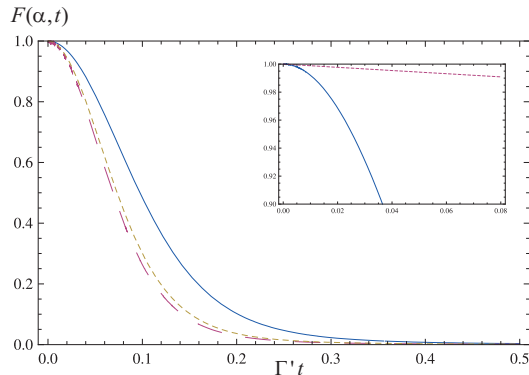


Figure 5: Fringe visibility for $r = \omega_c/\omega_0 = 0.1$ for the Ohmic (solid), super-Ohmic (dashed) and sub-Ohmic (dotted line) reservoirs. The inset shows the comparison between non-Markovian (solid line) and Markovian (dotted line) fringe visibility for the Ohmic reservoir. Plots are given in unitless time $\Gamma't = 2g^2\omega_0t$, where g is the coupling constant. We have set $k_B T/(\hbar\omega_0) = 100$.

with respect to the sub-Ohmic and super-Ohmic reservoirs, and in the case of $r = 10$ also with respect to the corresponding Markovian reservoir.

Our study of decoherence induced by different reservoir spectra gives an indication of which implementation (i.e., trapped ions, solid state devices, etc.) one should choose, in order to benefit from the naturally occurring environmental modes, like the typical sub-Ohmic $1/f$ -noise in solid state devices.

The second decoherence control technique, utilizing the so-called quantum Zeno effect, is based on the fact that initial non-Markovian decoherence rate is slower than the Markovian one for sufficiently small times.

7.2 The quantum Zeno effect

The quantum Zeno effect was originally introduced as the quantum Zeno paradox, because according to it, making certain types of measurements in rapid succession on a quantum state would, at least theoretically, result in completely freezing the dynamics. This is the reason why this effect received this name, as it reminded of the Greek philosopher Zeno's paradox about a sped arrow which is frozen in time in every frame along its trajectory [104]. Measurements that freeze the dynamics of the system are, in practise impossible to make [105], but it is known that the dynamics of an unstable system can indeed be slowed

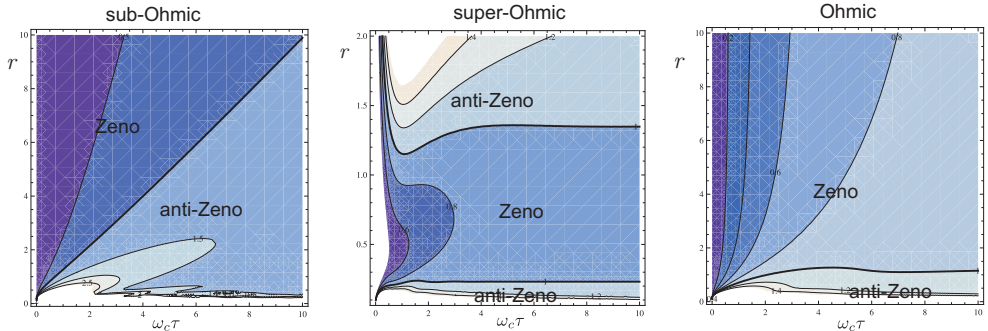


Figure 6: QZE/AZE -crossover for the sub-Ohmic, super-Ohmic and Ohmic high T reservoirs. We plot the ratio between the effective decay rate γ^Z and the Markovian decay rate γ^0 as a function of $r = \omega_c/\omega_0$ and of the measurement time interval $\omega_c\tau$.

down by making certain frequent measurements [106]. This is known as the quantum Zeno effect. Depending on the frequency of the measurements, and on some environmental factors, the decay dynamics can also be enhanced [107]. The latter effect is called the anti- or inverse-Zeno effect [108].

Quantum Zeno effect has been mostly studied for two-level systems, and an experiment with ^9Be -ions has verified the effect in 1990 [109]. Ten years later, the description for the quantum Zeno effect (QZE) and anti-Zeno effect (AZE) was given for the damped harmonic oscillator in an Ohmic reservoir [16, 110]. We have generalized these results to sub-Ohmic and super-Ohmic baths, and consequently found how extremely sensitive these effects are to the form of the environment.

The physics behind the QZE can be expressed in a rather simple way. Consider a two-level system, like two distinct energy levels. Let $P(\tau)$ denote the survival probability of the initial state after a short time τ , when the system is interacting with an environment of radiation modes. We can write this probability as $P(\tau) = \exp[-\gamma(\tau)\tau]$, where γ is the decay rate.

Each measurement querying the occupancy of each energy level projects the evolving state either to the initial excited state, or to ground state. If the measurements are sufficiently frequent, the system has very little time to decay, and hence the measurement will project the state to be the initial state with probability $\simeq 1$. After N measurements, performed at equal time intervals τ (where $t = N\tau$ is the duration of the experiment), the survival probability for the excited state reads $P(t) = P^N(t) = \exp[-\gamma(\tau)t]$.

For a quantum harmonic oscillator, we focus on an initial Fock state, $|n\rangle$. Performing N nonselective energy measurements at time intervals τ such that $P_n(\tau) = \langle n|\rho_S(\tau)|n\rangle \simeq 1$, we obtain an expression for the probability to find the system in its initial state $|n\rangle$ after a time t , in presence of measurements [108, 110]:

$$P_n^N(t) = P_n(\tau)^N \equiv \exp[-\gamma_n^Z(\tau)t], \quad (65)$$

where $\gamma_n^Z(\tau)$ is the effective decay rate. At high temperatures this rate is given by $\int_0^\tau \Delta(t') dt'/\tau$ and it is independent of n [110].

In absence of measurements, that is, assuming measurement time interval $\tau \rightarrow \infty$, one obtains the "undisturbed" decay rate

$$\gamma^0 = \lim_{\tau \rightarrow \infty} \gamma_n^Z(\tau) = \Delta_M. \quad (66)$$

To quantify the quantum Zeno effect we compare the the decay rates in presence and in absence of measurements. The quantity

$$\frac{\gamma_n^Z(\tau)}{\gamma_n^0} \simeq \frac{\int_0^\tau \Delta(t') dt'}{\tau \Delta_M} \quad (67)$$

characterizes the occurrence of either enhanced decay via AZE, or inhibited decay due to QZE. If $\gamma_n^Z(\tau)/\gamma^0 < 1$, the decay in presence of measurements is slower than the Markovian decay in absence of measurements, and quantum Zeno effect comes into play. On the other hand, if $\gamma_n^Z(\tau)/\gamma^0 > 1$, acceleration of the decay due to the measurements occurs (anti-Zeno effect). The crossover time τ^* separates these two regions.

We have found that under different reservoirs, the QZE/AZE-crossover time τ^* depends on the spectrum and resonance parameter value, as well as on the interval of time between measurements $\omega_c\tau$, in a very delicate way. A plot of the QZE/AZE-crossover is shown in Fig. 6, where a thicker black line represents the crossover between different dynamical scenarios.

One feature of the QZE–AZE dynamics is the fact that the dynamics can be extremely sensitive to the reservoir parameters. Consider the super-Ohmic reservoir, for example. There, two system oscillators with slightly different frequencies $\omega_0 \simeq \omega_c$ (correspondent, e.g., to $r = 1$ and $r = 1.5$) may act, in presence of measurements, in completely opposite ways, one showing mostly AZE ($r = 1.5$) and the other one only QZE ($r = 1$).

We found also that for small values of r the nonselective energy measurements always accelerate decoherence. The reason lies in the initial jolt of

the diffusion rate $\Delta(t)$, which causes a strong initial decoherence acting more rapidly than in the Markovian case.

In the trapped ion context, the non-selective energy measurements needed to obtain QZE or AZE, can be performed by simply switching the reservoir on and off [16].

8 Conclusions

In this Thesis I have presented my results on different aspects of the dynamics of the damped harmonic oscillator.

I have discussed the fundamental problem of quantum-to-classical transition. I have shown that different ways to characterize nonclassicality result in qualitatively and quantitatively different transition times for the emergence of classicality. Previously, decoherence causing the transition from quantum to classical was considered to occur faster for more macroscopically separated initial states. Our results challenge this view, since for almost all the nonclassicality indicators considered, an increase in the initial wave-packet separation does not necessarily shorten the decoherence time.

I have shown that the non-Markovian dynamics of different quantities such as energy dissipation, decoherence and squeezing, depend strongly on the spectral form of the environment coupled to the system. The analytic results I have obtained have allowed us to connect reservoirs strongly peaked in the low frequency realm ($\omega < \omega_0$) to more pronounced non-Markovian oscillations in the heating and squeezing dynamics. The sensitivity of the decay dynamics on the reservoir structure was further investigated in the context of decoherence control by means of engineered reservoirs and by modifying the system-reservoir coupling.

All these effects are very sensitive to the form of the spectrum, even on the thermalization time scales, sometimes changing the nature of the dynamics completely. Taking these effects into account in further experiments is therefore very important.

References

- [1] S. J. Freedman and J. F. Clauser, Phys. Rev. Lett. **28**, 938 (1972).
- [2] A. Aspect, P. Grangier, and G. Roger, Phys. Rev. Lett. **49**, 91 (1982).
- [3] R. Horodecki, P. Horodecki, M. Horodecki, and K. Horodecki, Rev. Mod. Phys. **81**, 865 (2009).
- [4] Monroe, C., Meekhof, D. M., King, B. E., and Wineland, D. J., Science **272**, 1131 (1996).
- [5] M. Arndt, O. Nairz, J. Vos-Andreae, C. Keller, G. van der Zouw and A. Zeilinger, Nature **401**, 680 (1999).
- [6] M. Schlosshauer, *Decoherence and the quantum-to-classical transition*, (Springer-Verlag, Berlin, 2007).
- [7] H.-P. Breuer and F. Petruccione, *The Theory of Open Quantum Systems* (Oxford University Press, Oxford, 2002).
- [8] T. Quang, M- Woldeyohannes, S. John, and G. S. Agarwal, Phys. Rev. Lett. **79**, 5238 (1997).
- [9] J. J. Hope, G. M. Moy, M. J. Collett, and C. M. Savage, Phys. Rev. A **77**, 032117 (2008).
- [10] F. Intravaia, S. Maniscalco, and A. Messina, Phys. Rev. A **67**, 042108 (2003).
- [11] T. Yu and J. H. Eberly, Science **323**, 598 (2009).
- [12] E.-M. Laine, J. Piilo, and H.-P. Breuer, Phys. Rev. A **81**, 062115 (2010).
- [13] R. Vasile, S. Maniscalco, M. G. A. Paris, H.-P. Breuer, J. Piilo, Phys. Rev. A **84**, 052118 (2011).
- [14] Á. Rivas, S. F. Huelga, and M. B. Plenio, Phys. Rev. Lett. **105**, 050403 (2010).
- [15] M. M. Wolf, J. Eisert, T. S. Cubitt, and J. I. Cirac, Phys. Rev. Lett. **101**, 150402 (2008).
- [16] S. Maniscalco, Laser Physics, Vol. 20, No. 5, 1251 (2010).

- [17] U. Weiss, *Quantum Dissipative Systems*, 3rd ed. (World Scientific, Singapore, 2008).
- [18] C.W. Gardiner and P. Zoller, *Quantum Noise* (Springer-Verlag, Berlin, 2010).
- [19] C.W. Lai, P. Maletinsky, A. Badolato, and A. Imamoglu, Phys. Rev. Lett. **96**, 167403, (2006).
- [20] A. Pomyalov and D. J. Tannor, J. Chem. Phys. **123**, 204111 (2005).
- [21] P. Hänggi, P. Talkner, and M. Borkovec, Rev. Mod. Phys. **62**, 251 (1990).
- [22] J. Piilo, S. Maniscalco, K. Härkönen, and K.-A. Suominen, Phys. Rev. Lett. **100**, 180402 (2008).
- [23] J. Piilo, K. Härkönen, S. Maniscalco, and K.-A. Suominen, Phys. Rev. A **79**, 062112 (2009).
- [24] B. Misra and E. C. G. Sudarshan, J. Math. Phys. **18**, 756 (1977).
- [25] G. Lindblad, Commun. Math. Phys. **48**, 119 (1976).
- [26] V. Gorini, A. Kossakowski, and E. Sudarshan, J. Math. Phys. **17**, 821 (1976).
- [27] A. Jamiolkowski, Rep. Math. Phys. **3**, 275 (1972).
- [28] M. D. Choi, Linear Alg. and Appl. **10**, 285 (1975).
- [29] B. L. Hu, J. P. Paz, and Y. Zhang, Phys. Rev. D **45**, 2843 (1992).
- [30] F. Intravaia, S. Maniscalco, and A. Messina, Eur. Phys. J. B **32**, 97 (2003).
- [31] S. Maniscalco, J. Piilo, and K.-A. Suominen, Eur. Phys. J. D **55**, 181 (2009).
- [32] D. Chruscinski and A. Kossakowski, Phys. Rev. Lett. **104**, 070406 (2010).
- [33] M. S. Kim, W. Son, V. Buzek, and P. L. Knight, Phys. Rev. A **65**, 032323 (2002).
- [34] Wang Xiang-bin, Phys. Rev. A **66**, 024303 (2002).

- [35] M. A. Nielsen and I. L. Chuang, *Quantum Computation and Quantum Information*, (Cambridge, Cambridge University Press, 2000).
- [36] E. P. Wigner, Phys. Rev. **40**, 749 (1932).
- [37] K. E. Cahill and R. J. Glauber, Phys. Rev. **177**, 1882 (1969).
- [38] N. Lütkenhaus and S. M. Barnett, Phys. Rev. A **51**, 3340 (1995).
- [39] C. T. Lee, Phys. Rev. A **44**, R2775 (1991).
- [40] R. J. Glauber, Phys. Rev. **131**, 2766 (1963).
- [41] E. C. G. Sudarshan, Phys. Rev. Lett. **10**, 277 (1963).
- [42] U. M. Titulaer and R. J. Glauber, Phys. Rev. **140**, B676 (1965).
- [43] D. N. Klyshko, Phys. Lett. A **213**, 7 (1996).
- [44] W. Vogel, Phys. Rev. Lett. **84**, 1849 (2000).
- [45] Th. Richter and W. Vogel, Phys. Rev. Lett. **89**, 283601 (2002).
- [46] J. K. Korbicz, J. I. Cirac, J. Wehr, and M. Lewenstein, Phys. Rev. Lett. **94**, 153601 (2005).
- [47] J. K. Asbóth, J. Calsamiglia, and H. Ritsch, Phys. Rev. Lett. **94**, 173602 (2005).
- [48] R. Egger, H. Grabert, and U. Weiss, Phys. Rev. E **55**, R3809 (1997).
- [49] L. Mandel, Opt. Lett. **4**, 205 (1979).
- [50] M. Hillery, Phys. Rev. A **35**, 725 (1987).
- [51] I. P. Degiovanni, M. Genovese, V. Schettini, M. Bondani, A. Andreoni, M. G. A. Paris, Phys. Rev. A **79**, 063836 (2009).
- [52] A. Miranowicz, M. Bartkowiak, X. Wang, Y. X. Liu, and F. Nori Phys. Rev. A **82**, 013824 (2010).
- [53] J. Solomon Ivan, S. Chaturvedi, E. Ercolessi, G. Marmo, G. Morandi, N. Mukunda, and R. Simon, e-print: arXiv:1009.6104v1
- [54] G. Brida, M. Bondani, I. P. Degiovanni, M. Genovese, M. G. A. Paris, I. Ruo Berchera, and V. Schettini, Found. Phys. **41**, 305 (2011).

- [55] E. Schrödinger, *Naturwissenschaften* **23**, 807, 823, 844 (1935); reprinted in english in *Quantum Theory of Measurement*, J. A. Wheeler and W. H. Zurek, Princeton University Press, (Princeton, NJ) 1983.
- [56] J. B. Paz and W. H. Zurek, in *Coherent Matter Waves*, Proceedings of the 72nd Les Houches Summer School (Springer-Verlag, Berlin, 1999).
- [57] W. H. Zurek, *Physics Today* **44** (10), 36 (1991).
- [58] J. P. Paz, S. Habib, and W. H. Zurek, *Phys. Rev. D* **47**, 488 (1993).
- [59] M. Brune, E. Hagley, J. Dreyer, X. Maitre, A. Maali, C. Wunderlich, J. M. Raimond, and S. Haroche, *Phys. Rev. Lett.* **77**, 4887 (1996).
- [60] C. Monroe, D. M. Meekhof, B. E. King, and D. J. Wineland, *Science* **272**, 1131 (1996).
- [61] S. Deleglise, I. Dotsenko, C. Sayrin, J. Bernu, M. Brune, J. M. Raimond, and S. Haroche *Nature* **455**, 510 (2008).
- [62] S. Maniscalco, J. Piilo, and K.-A. Suominen, *Eur. Phys. J. D* **55**, 181 (2009).
- [63] C. J. Myatt, B. E. King, Q. A. Turchette, C. A. Sackett, D. Kielpinski, W. M. Itano, C. Monroe and D. J. Wineland, *Nature* **403**, 269 (2000).
- [64] M. G. A. Paris and J. Rehacek Eds., *Quantum State Estimation*, Lecture Notes in Physics, **649** (Springer, Heidelberg, 2004).
- [65] L. Diósi, *Phys. Rev. Lett.* **85**, 2841 (2000).
- [66] A. I. Lvovsky and J. H. Shapiro, *Phys. Rev. A* **65**, 033830 (2002).
- [67] S. M. Barnett and P. M. Radmore, *Methods in Theoretical Quantum Optics*, (Oxford University Press, Oxford, 1997).
- [68] G. M. D'Ariano, M. F. Sacchi, and P. Kumar, *Phys. Rev. A* **59**, 826 (1999).
- [69] M. Munroe, D. Boggavarapu, M. E. Anderson, and M. G. Raymer, *Phys. Rev. A* **52**, R924 (1995); Y. Zhang, K. Kasai, and M. Watanabe, *Opt. Lett.* **27**, 1244 (2002).

- [70] A. R. Rossi, S. Olivares, M. G. A. Paris, Phys. Rev. A **70**, 055801 (2004); G. Zambra, A. Andreoni, M. Bondani, M. Gramegna, M. Genovese, G. Brida, A. Rossi, and M. G. A. Paris, Phys. Rev. Lett. **95**, 063602 (2005).
- [71] G. Zambra, M. Bondani, A. S. Spinelli, and A. Andreoni, Rev. Sci. Instrum. **75**, 2762 (2004).
- [72] A. Fukasawa, J. Haba, A. Kajeyama, H. Nakazawa, and M. Suyama, IEEE Trans. Nucl. Sci. **55**, 758 (2008).
- [73] M. Wilkens and P. Meystre, Phys. Rev. A **43**, 3832 (1991).
- [74] S. Wallentowitz and W. Vogel, Phys. Rev. Lett. **75**, 2932 (1995).
- [75] A. Mari, K. Kieling, B. M. Nielsen, E. S. Polzik, and J. Eisert, Phys. Rev. Lett. **106**, 010403 (2011).
- [76] T. Yu and J. H. Eberly, Phys. Rev. Lett. **93**, 140404 (2004).
- [77] X.-M. Lu, X. Wang, and C. P. Sun, Phys. Rev. A **82**, 042103 (2010).
- [78] H.-P. Breuer et al. Phys. Rev. Lett. **103**, 210401 (2009).
- [79] Q. A. Turchette, C. J. Myatt, B. E. King, C. A. Sackett, D. Kielpinski, W. M. Itano, C. Monroe, and D. J. Wineland, Phys. Rev. A **62**, 053807 (2000).
- [80] B. B. Blinov, D. L. Moehring, L.-M. Duan, and C. Monroe, Nature **428**, 153 (2004).
- [81] M. Bayer et al., Phys. Rev. B **65**, 195315 (2002).
- [82] I. Chiorescu, Y. Nakamura, C.J.P.M. Harmans, and J.E. Mooij, Science **299**, 1869 (2003).
- [83] D. I. Schuster et al., Phys. Rev. Lett. **94**, 123602 (2005).
- [84] J.-I. Yoshikawa, T. Hayashi, T. Akiyama, N. Takei, A. Huck, U. L. Andersen, and A. Furusawa *Phys. Rev. A* **76**, 060301(R) (2007).
- [85] J.-I. Yoshikawa, Y. Miwa, A. Huck, U. L. Andersen, P. van Loock, and A. Furusawa *Phys. Rev. Lett.* **101**, 250501 (2008).
- [86] B.E. Kane, Nature **393**, 133 (1998).

- [87] J. I. Cirac and P. Zoller, Phys. Rev. Lett. **74**, 4091 (1995).
- [88] J. M. Martinis, Quantum Inf. Process **8**, 81 (2009).
- [89] R. P. Feynman, Int. J. Theor. Phys. **21**, 467 (1982).
- [90] M. Kliesch, T. Barthel, C. Gogolin, M. Kastoryano, and J. Eisert, Phys. Rev. Lett. **107**, 120501 (2011).
- [91] J. Piilo and S. Maniscalco, Phys. Rev. A **74**, 032303 (2006).
- [92] H. Paul, *Introduction to Quantum Optics From Light Quanta to Quantum Teleportation* (Cambridge University Press, Cambridge, 2004).
- [93] S. Maniscalco, J. Opt. B: Quantum Semiclass. Opt. **7**, S398 (2005).
- [94] K. Matsuo, Phys. Rev. A **47**, 3337 (1993).
- [95] P. G. Kwiat, A. J. Berglund, J. B. Altepeter and A. G. White, Science **290**, 498 (2000).
- [96] P. Facchi, S. Tasaki, S. Pascazio, H. Nakazato, A. Tokuse, and D. A. Lidar, Phys. Rev. A **71** 022302 (2005).
- [97] G. Gordon, G. Kurizki, and D. A. Lidar, Phys. Rev. Lett. **101**, 010403 (2008).
- [98] S. John and T. Quang, Phys. Rev. Lett. **74**, 3419 (1995).
- [99] S. John and T. Quang, Phys. Rev. Lett. **78**, 1888 (1997).
- [100] T. Quang, M. Woldeyohannes, and S. John, Phys. Rev. Lett. **79**, 5238 (1997).
- [101] S. Haroche and J.-M. Raimond, *Exploring the Quantum*, (Oxford University Press, Oxford, 2006).
- [102] T. Tanabe, M. Notomi, H. Taniyama, and E. Kuramochi, Phys. Rev. Lett. **102**, 043907 (2009).
- [103] M. J. Biercuk, H. Uys, A. P. VanDevender, N. Shiga, W. M. Itano, and J. J. Bollinger, Nature **458**, 996 (2009).
- [104] B. Misra and B. E. Sudarshan, J. Math. Phys. **18**, 756 (1977).

- [105] H. Nakazato, M. Namiki, S. Pascazio and H. Rauch, *Phys. Lett. A* **199**, 27 (1995).
- [106] P. Facchi and S. Pascazio, *Progress in Optics*, ed. E. Wolf (Elsevier, Amsterdam, 2001), Vol. 42, Chap. 3, p. 147.
- [107] P. Facchi and S. Pascazio, *J. Phys. A: math. theor.* **41**, 493001 (2008).
- [108] P. Facchi, H. Nakazato, and S. Pascazio, *Phys. Rev. Lett.* **86**, 2699 (2001).
- [109] W. M. Itano, D. J. Heinzen, J. J. Bollinger and D. J. Wineland, *Phys. Rev. A* **41**, 2295 (1990).
- [110] S. Maniscalco, J. Piilo, and K.-A. Suominen, *Phys. Rev. Lett.* **97**, 130402 (2006).